

Electricity Generation from Synthetic Acid-Mine Drainage (AMD) Water using Fuel Cell Technologies

SHAOAN CHENG, BRIAN A. DEMPSEY,
AND BRUCE E. LOGAN*

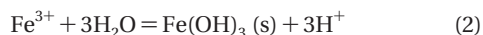
Department of Civil and Environmental Engineering, The
Pennsylvania State University, University Park,
Pennsylvania 16802, U.S.A

Received May 23, 2007. Revised manuscript received August
27, 2007. Accepted September 12, 2007.

Acid-mine drainage (AMD) is difficult and costly to treat. We investigated a new approach to AMD treatment using fuel cell technologies to generate electricity while removing iron from the water. Utilizing a recently developed microbial fuel cell architecture, we developed an acid-mine drainage fuel cell (AMD-FC) capable of abiotic electricity generation. The AMD-FC operated in fed-batch mode generated a maximum power density of 290 mW/m² at a Coulombic efficiency greater than 97%. Ferrous iron was completely removed through oxidation to insoluble Fe(III), forming a precipitate in the bottom of the anode chamber and on the anode electrode. Several factors were examined to determine their effect on operation, including pH, ferrous iron concentration, and solution chemistry. Optimum conditions were a pH of 6.3 and a ferrous iron concentration above ~0.0036 M. These results suggest that fuel cell technologies can be used not only for treating AMD through removal of metals from solution, but also for producing useful products such as electricity and recoverable metals. Advances being made in wastewater fuel cells will enable more efficient power generation and systems suitable for scale-up.

Introduction

Acid-mine drainage (AMD) is a serious environmental problem caused by the biological oxidation of metal sulfides to metal sulfates. AMD is toxic to aquatic life because of its low pH and the solubilization of metals such as lead, copper, cadmium, and arsenic. The goals of AMD treatment are to raise the pH of the water and to achieve controlled removal of iron and other metals. Increasing the pH and provision of an oxidizing agent result in iron precipitation, which is shown by the following two reactions:



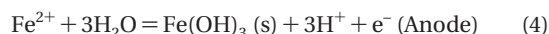
Passive treatment of AMD is accomplished through an increase of pH (1, 2), oxygen transfer (3), and precipitation and sedimentation of Fe(III) (hydr)oxides, along with biological processes for effluent polishing that also accomplish Mn(II) removal (4–7). Active treatment often involves a rapid increase in pH (lime, caustic, or other base) followed by agitation and forced aeration. Electrolytic oxidation processes have also been used (8, 9). Although these methods are

effective, they can be costly, and recovery of ferric oxides for reuse is difficult (10, 11). Thus, conventional passive and active processes typically provide no other immediate benefit other than treatment.

It is proposed here that AMD can be treated using new types of fuel cells being developed to generate electricity from wastewater. Typical fuel cells generate electricity from gases or liquid fuels such as hydrogen or methanol. However, new types of microbial fuel cells (MFCs) have been developed that are suitable for generating electricity from the bacterial oxidation of organic matter such as acetate, glucose, and domestic wastewater (12–22), and inorganic matter such as sulfides (23). The first requirement for using a fuel cell is that the overall reaction is energetically favorable. When ferrous iron is oxidized with oxygen, the overall reaction is that shown in eq 3:



Under standard conditions ([H⁺] = 1 M, pH = 0), this reaction is thermodynamically favorable, but it has a small free energy ($\Delta G^\circ = -27.15$ kJ/mol). This reaction is strongly pH dependent, however, and therefore, increasing the pH makes the reaction more favorable. The overall reaction can be split into two half-cell reactions that can separately occur at the anode and cathode of a fuel cell, as shown by eqs 4 and 5:



If AMD is treated using a fuel cell, ferrous iron is oxidized to ferric iron at the anode and precipitated (eq. 4), and O₂ is reduced to water at the cathode (eq. 5) at an overall voltage of $E_{\text{cell}}^0 = 0.28$ V under standard conditions. The voltage under nonstandard conditions is given by eq 6,

$$E = E_{\text{cell}}^0 - \frac{RT}{nF} \ln \frac{[\text{H}^+]^2}{[\text{Fe}^{2+}]\text{P}_{\text{O}_2}} \quad (6)$$

where E is the cell voltage, R is the universal gas constant, T is the temperature of the electrolyte, P_{O_2} is the partial pressure of oxygen, and [H⁺] and [Fe²⁺] are the activities of H⁺ and Fe²⁺ in solution, respectively. Assuming conditions (used in these experiments) of pH = 6.3, $\text{P}_{\text{O}_2} = 0.21$ atm, $T = 303$ K, and [Fe²⁺] = 7×10^{-3} M, the cell voltage could reach 0.899 V for hydrous ferric oxide (HFO) and a slightly greater voltage for goethite.

The current generated in a fuel cell process cannot be predicted because of overpotentials at the electrodes and changes in solution chemistry in the cells and at the electrode surface. To demonstrate the feasibility of this new type of AMD fuel cell (AMD-FC) treatment process, we therefore examined the treatment of a synthetic AMD solution using a two-chambered MFC previously developed for electricity generation from domestic wastewater (24). We demonstrate here that we can achieve complete Fe²⁺ removal and that we can generate electricity at power densities slightly lower than those achieved with organic substrates and bacteria. Several factors that could affect power production were examined, including pH, ferrous iron concentration, and solution chemistry.

Experimental Section

Fuel Cell Construction. The AMD-FCs were constructed based on a previous MFC design (24) from two plastic (Plexiglas) cylindrical chambers each 2 cm long by 3 cm in

* Corresponding Author: Phone: 814-863-7908; Fax: 814-863-7304; E-mail: blogan@psu.edu.

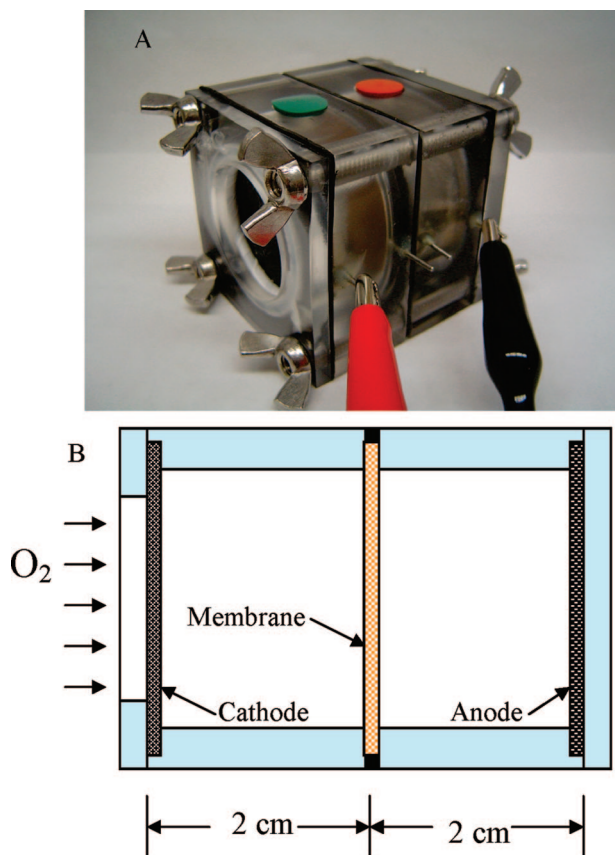


FIGURE 1. Laboratory-scale prototype (A) and schematic (B) fuel cell system used to generate electricity.

diameter (14 mL liquid volume of each chamber) separated by an anion exchange membrane (AMI7001, membrane international Inc., New Jersey). The anode was carbon cloth (non wet-proofed, type A, E-TEK) with a projected surface area of 7 cm² (one side). The cathode electrode was made by applying Pt (0.5 mg/cm²) to a commercially available carbon cloth (Type B, E-TEK, 30 wt % wet-proofed) (17). The membrane was held between the two cylindrical chambers with a rubber O-ring to prevent leakage. The anode electrode was located at the end of one chamber and covered with a plastic end plate (5 × 5 × 0.6 cm). The cathode electrode was placed at the end of another chamber and covered with another end plate with a center hole (3 cm in diameter), with the Pt-catalyst side facing to the solution and another side to air (Figure 1). Platinum wires (1 mm in diameter) were used to connect both electrodes and used as terminals of the cell.

Anode and Cathode Solutions. The catholyte contained NaCl (to increase solution conductivity) and NaHCO₃ (pH buffer), whereas the anolyte also contained FeSO₄. Before FeSO₄ was added, both the anolyte and catholyte solutions were sparged with CO₂ (except where stated otherwise) for 0.5 h to adjust the pH and remove dissolved oxygen. The pH was further adjusted to 6.3 (except where noted) with HCl under conditions of continuous CO₂ sparging.

AMD-FC Operation. The reactor was filled with electrolytes in an anaerobic glovebox and then removed and placed in a temperature controlled room (30 °C). The reactor was operated in open circuit mode for 0.5 h before connecting an external resistor (1000 Ω in all experiments except where noted) to measure electricity generation. The reactor was first operated with a medium containing 0.1 M NaCl and 0.02 M NaHCO₃ with sparging of different gases (N₂ and CO₂) to investigate the effects of sparging on power generation or without sparging as indicated. The concentration of Fe²⁺

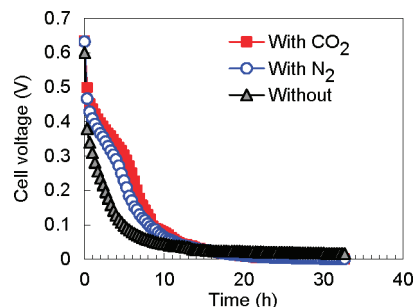


FIGURE 2. Electricity generation from the solution pretreated with different gases. Conditions; 0.1 M NaCl, 0.02 M NaHCO₃, 0.007 M Fe²⁺, pH 6.3, and 1000 Ω external resistor.

was 0.007 M, except where noted. To determine the effect of various conditions on power generation, pH (4–7.5) and concentrations of sodium bicarbonate (0–0.1 M), potassium chloride (0–0.3 M), and ferrous iron (0.001–0.018 M) were varied. Experiments were conducted in duplicate.

Analyses. The voltage across the external resistor in the circuit of the fuel cell was recorded at 20 min intervals using a multimeter (Keithley instruments, Ohio) connected to a personal computer. Current (*I*) and power ($P = IV$) were calculated as previously described (15), with the power density normalized by the projected surface area of one side of the anode. Power density was calculated using the measured cell voltages averaged over the first three hours of initial reactor operation. Coulombic efficiency (CE) was calculated as: $CE = C_p/C_{th} \times 100\%$, where C_p is the total coulombs calculated by integrating the current over time, and C_{th} is the theoretical amount of coulombs that can be produced from the added Fe²⁺. Polarization curves were obtained by measuring the voltage (averaged voltage over the initial 3 h) generated at various external resistances and then used to evaluate the maximum power density (25).

Fe²⁺ was measured using a ferrozine-based colorimetric method (26). The sample (0.1 mL) was diluted into 5 mL of 0.5 N HCl. After 15 min, 0.1 mL of the diluted sample was added to 5 mL of ferrozine (1 g/L) in 50 mM 4-(2-hydroxyethyl)-1-piperazineethanesulfonic acid (HEPES) buffer, and Fe²⁺ was quantified using a spectrophotometer at 562nm.

Results

Voltage Generation and Effect of Gas Sparging. The measured open circuit voltage (OCV) of the cell was 0.63 V. When the external resistor was connected, the cell voltage immediately decreased to 0.48 V and then gradually fell to 0 V over the next 25 h as the iron was oxidized (Figure 2). Sparging with different gases, or the absence of sparging, did not affect the OCV at pH 6.3, but it did affect power generation and CE (Figure 2). Without gas sparging, the maximum power density was 114 mW/m² (2.85 W/m³; total reactor volume) with CE = 76%. Power density increased to 222 mW/m² with N₂ sparging and to 256 mW/m² with CO₂ sparging. The CEs were also higher, with 87% for N₂ sparging and 97.8% for CO₂ sparging. On the basis of these results, CO₂ gas sparging was used before all other experiments.

A red precipitate was observed on the bottom of the anode chamber and on the anode surface following each batch cycle of operation. X-ray diffraction (XRD) analysis indicated the dried precipitate was partially goethite (α-FeOOH), which is produced from HFO during drying and storage of AMD solids. No Fe²⁺ was detected in either chamber at the end of the batch cycle, indicating that Fe²⁺ was completely oxidized to Fe³⁺.

NaHCO₃ and KCl. NaHCO₃ was added to the medium containing 400 mg/L Fe²⁺, NaCl (0.1 M), and at an initial pH of 6.3, to test the effect of the pH buffer capacity on power

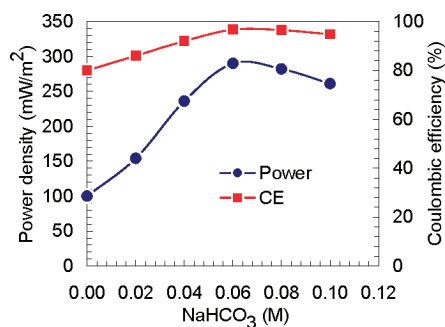


FIGURE 3. Effect of NaHCO_3 on power density and CE.

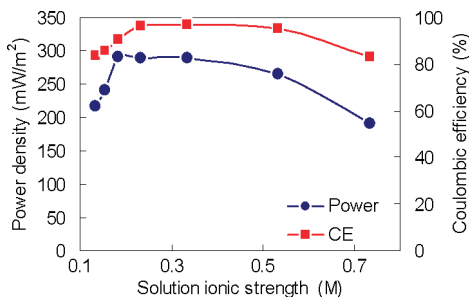


FIGURE 4. Effect of solution-ionic strength on power density and CE.

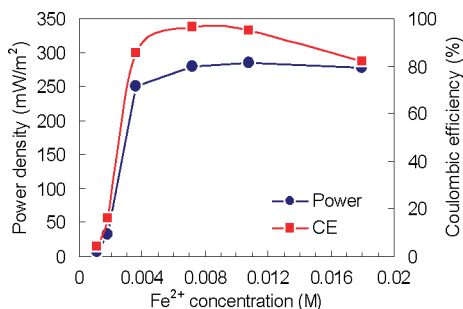


FIGURE 5. Effect of Fe^{2+} concentration on power and CE.

generation. Without NaHCO_3 , the maximum power produced was 100 mW/m^2 . The addition of NaHCO_3 increased the maximum power to 290 mW/m^2 up to a concentration of 0.06 M , and then it decreased with further NaHCO_3 addition to 0.1 M (Figure 3). The CE followed a similar trend, with a maximum of $\text{CE} = 96.7\%$ at 0.06 M NaHCO_3 . After each run, the final pH was 3.4 ± 0.2 in the absence of NaHCO_3 , 5.8 ± 0.2 with 0.02 M , 6.2 ± 0.1 with 0.04 M , and 6.4 ± 0.2 with $\geq 0.06 \text{ M}$ of NaHCO_3 .

KCl was added to determine the effect of solution-ionic strength (IS) on power generation (27) at a fixed concentration of 0.06 M NaHCO_3 . The power density increased from 216 to 290 mW/m^2 as the IS was increased from 0.134 to 0.184 M (Figure 4). The power density then decreased to 190 mW/m^2 as the IS was further increased to 0.784 M . The CE increased from 85 to 97% when the IS was increased from 0.134 to 0.184 M , and then it decreased to 85% at an IS of 0.584 M .

Fe^{2+} Concentration. The Fe^{2+} concentration was varied from 0.001 to 0.018 M in a medium containing optimal concentrations of NaHCO_3 (0.06 M) and KCl (0.05 M). At 0.001 M Fe^{2+} , the power density was 8 mW/m^2 (Figure 5) and increased to 250 mW/m^2 as the concentration of Fe^{2+} was increased to 0.0036 M . The power density further increased to 290 mW/m^2 at a Fe^{2+} concentration of 0.007 M , but it did not further increase at higher Fe^{2+} concentrations. The CE increased from 4% to $85\text{--}96\%$ as the Fe^{2+} concentration was increased from 0.001 to 0.0036 M .

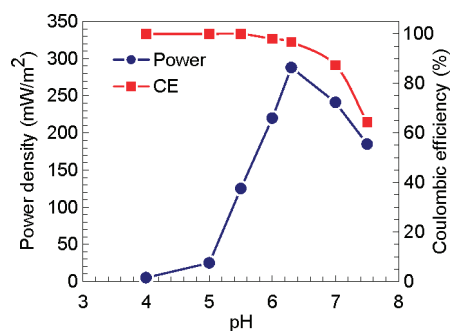


FIGURE 6. Effect of pH on power density and CE.

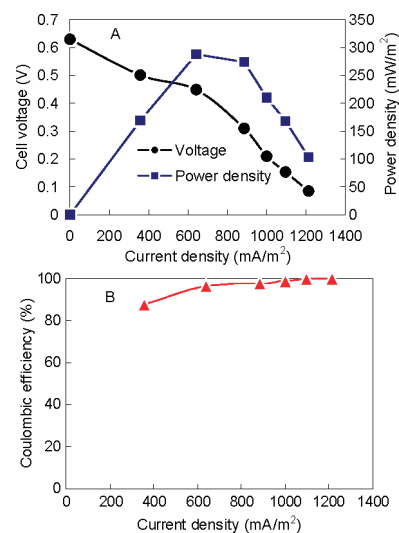


FIGURE 7. Power density (A) and Coulombic efficiency (B) as function of current density.

pH. To determine the effect of pH, we examined power generation and CE using a medium containing 0.06 M NaHCO_3 , 0.05 M KCl , and 0.007 M Fe^{2+} . The pH was varied from 4 to 7.5 by adding HCl or NaOH . An optimal power production of 290 mW/m^2 was achieved at a pH of 6.3, with power decreasing to <250 at pH = 5 and to 185 mW/m^2 at pH = 7.5 (Figure 6). The CEs decreased from 100% at pH = 4 to 96.7% at pH = 6.3 and then to 64% at a pH = 7.5. The pH of the anolyte decreased over the course of the experiments by $5\text{--}10\%$, except for the experiment at pH 6.3, where the pH was constant.

Maximum Power and Current Densities. The maximum power that could be produced in the system was determined by varying the circuit resistance from 100 to 2000Ω , under the optimal conditions identified above (0.06 M NaHCO_3 , 0.05 M KCl , 0.007 M Fe^{2+} , and pH = 6.3). The maximum power was 290 mW/m^2 (7.2 W/m^3 total reactor volume) at a current density of 640 mA/m^2 for an external resistance of 1000Ω (Figure 7A). The CE increased from 87 to 100% when the current density increased from 350 to 1200 mA/m^2 (Figure 7B).

Discussion

Ferrous iron was completely removed by conversion to insoluble ferric iron in the anode chamber of the AMD-FC, while simultaneously generating up to 290 mW/m^2 (7.2 W/m^3). Fe^{3+} oxides were precipitated on the anode, but the oxide layer remains conductive, as reported by Williams and Scherer (31) and confirmed by us at the end of an experiment using a multimeter (data not shown). Thus, the process was sustainable, as shown by continuous operation in fed-batch mode for over 42 days without a significant reduction in the

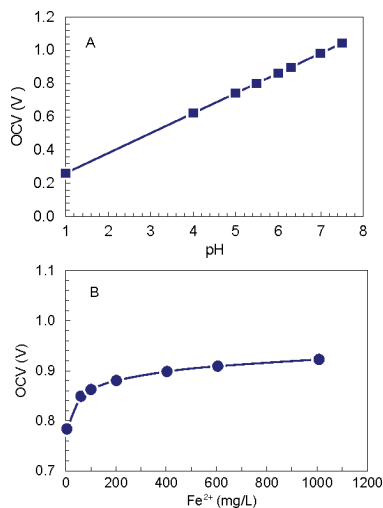


FIGURE 8. Theoretical open circuit voltage changes of AMD-FC (A) as a function of pH vs pH = 1 at 0.007 M Fe²⁺ and (B) as a function of Fe²⁺ concentration vs Fe²⁺ concentration = 1 M at pH 6.3, both at 0.06 M NaHCO₃, 0.05 M KCl, and P_{O₂} = 0.21 atm, T = 303 K.

capacity for power generation. The electricity produced by this process could be used at remote sites either for powering pumps or other control systems, or for monitoring the process (28–30). The iron is recoverable as a precipitate either on the anode or settled in the bottom of the anode chamber. The high CE and complete Fe²⁺ removal from the solution makes this AMD-FC treatment process useful both as a treatment process and as a method of electricity production. In addition, iron recovered in passive AMD treatment systems, following purification by additional treatment, can have additional market value as a pigment for paints or other uses (11). Thus, the system may also be considered as a metal recovery process.

The power density was influenced by Fe²⁺ concentration and pH, in a manner generally consistent with the trends expected from analysis using the Nernst equation. According to equation 6, cell voltage should increase with pH (Figure 8A); this was observed in experiments at pH < 6.3, although it was not observed at higher pH values (Figure 6). According to the Nernst equation, the maximum possible voltage increases with Fe²⁺ concentration (Figure 8B), and an increase in voltage with iron concentration was observed here (Figure 5). For example, increasing Fe²⁺ from 0.002 to 0.018 M increased the cell voltage from 464 to 650 mV, and it increased power output from 33 to 280 mW/m² (Figure 5). Above a pH of 6.3, power output decreased for reasons that are not well understood, but this decrease may be a result of oxygen transfer into the anode chamber (3, 31, 32). As the current and power decrease, the total mass of oxygen that diffuses into the chamber increases because of the increased duration of the fed-batch cycle. This decreases the CE, as shown in Figure 6, but it may also affect power due to an increase in the redox potential in the anode chamber.

The power generated here from iron oxidation was about 48% of that produced using acetate as a substrate for bacteria (610 mW/m², (24)). The CE measured here (over 97% under optimal conditions) was much larger than that obtained with this system using bacteria and acetate (72%). The system used here is a very basic type of MFC that has been used to examine factors that can increase power generation in these types of applications. However, the development of an economical treatment system will require the use of non-precious metal cathode catalysts and a system architecture that is scalable. Substantial progress has been made with MFCs in both of these areas. For example, the precious metal

(Pt) cathode catalyst used for oxygen reduction could be replaced with a transition metal (Cobalt) catalyst (17, 33). Scalable architectures for MFCs have been developed that are based on using graphite brush anodes and tubular membrane cathodes to provide increased surface areas per volume of reactor (34, 35). The use of these materials in AMD-FC reactors should enable scalable and more efficient systems for power generation and AMD treatment.

Acknowledgments

This research was supported by NSF Grant BES-0401885.

Literature Cited

- Hedin, R. S.; Watzlaff, G. R.; Nairn, R. W. Passive treatment of acid mine drainage with limestone. *J. Environ. Qual.* **1994**, *23*, 1338–1345.
- Cravotta, C. A. Size and performance of anoxic limestone drains to neutralize mine drainage. *J. Environ. Qual.* **2003**, *32*, 1277–1289.
- Dempsey, B. A.; Roscoe, H. C.; Ames, R.; Hedin, R.; Jeon, B.-H. Ferrous oxidation chemistry in passive abiotic systems for treatment of mine drainage. *Geochem.: Explor., Environ., Anal.* **2001**, *1*, 81–88.
- Olem, H.; Unz, R. F. Acid mine drainage treatment with rotation biological contactor. *Biotechnol. Bioeng.* **1977**, *19*, 1475–1491.
- Nermati, M.; Webb, C. A kinetic model for biological oxidation of ferrous iron by *Thiobacillus ferrooxidans*. *Biotechnol. Bioeng.* **1997**, *53*, 476–486.
- Nermati, M.; Harrison, S. T. L.; Hansford, G. S.; Webb, C. Biological oxidation of ferrous sulphate by *Thiobacillus ferrooxidans*: a review on the kinetic aspects. *Biochem. Eng. J.* **1998**, *1*, 171–190.
- Neclulita, C. M.; Zagury, G. J.; Bussiere, B. Passive treatment of acid mine drainage in bioreactors using sulfate-reducing bacteria: Critical review and research needs. *J. Environ. Qual.* **2007**, *36*, 1–16.
- Bunce, N. J.; Chartrand, M. M. G.; Keech, P. Electrochemical treatment of acidic aqueous ferrous sulfate and copper sulfate as models for acid mine drainage. *Wat. Res.* **2001**, *35*, 4410–4416.
- Chartrand, M. M. G.; Bunce, N. J. Electrochemical remediation of acid mine drainage. *J. Appl. Electrochem.* **2003**, *33*, 259–264.
- Dempsey, B. A.; Jeon, B. H. Characteristics of sludge produced from passive treatment of mine drainage. *Geochem.: Explor. Environ. Anal.* **2001**, *1*, 89–94.
- Kairies, C. L.; Capo, C. L.; Watzlaf, G. R. Chemical and physical properties of iron hydroxide precipitates associated with passively treated coal mine drainage in the Bituminous Regions of PA and MD. *Appl. Geochem.* **2005**, *20*, 1445–1460.
- Allen, R. M.; Bennetto, H. P. Microbial Fuel-Cells: electricity production from carbohydrates. *Appl. Biochem. Biotechnol.* **1993**, *39/40*, 27–40.
- Kim, H. J.; Park, H. S.; Hyun, M. S.; Chang, I. S.; Kim, M.; Kim, B. H. A mediator-less microbial fuel cell using a metal reducing bacterium, *Shewanella putrefaciens*. *Enzyme. Microbiol. Tech.* **2002**, *30*, 145–152.
- Liu, H.; Ramnarayanan, R.; Logan, B. E. Production of electricity during wastewater treatment using a single chamber microbial fuel cell. *Environ. Sci. Technol.* **2004**, *38*, 2281–2285.
- Cheng, S.; Liu, H.; Logan, B. E. Increased power generation in a continuous flow MFC with advective flow through the porous anode and reduced electrode spacing. *Environ. Sci. Technol.* **2006**, *40*, 2426–2432.
- Cheng, S.; Logan, B. E. Ammonia treatment of carbon cloth anodes to enhance power generation of microbial fuel cells. *Electrochem. Commun.* **2006**, *9*, 492–496.
- Cheng, S.; Liu, H.; Logan, B. E. Power densities using different cathode catalysts (Pt and CoTMPP) and polymer binders (Nafion and PTFE) in single chamber microbial fuel cells. *Environ. Sci. Technol.* **2006**, *40*, 364–369.
- Liu, H.; Cheng, S.; Logan, B. E. Production of electricity from acetate or butyrate in a single chamber microbial fuel cell. *Environ. Sci. Technol.* **2005**, *39*, 658–662.
- Bond, D. R.; Holmes, D. E.; Tender, L. M.; Lovley, D. R. Electrode-reducing microorganisms that harvest energy from marine sediments. *Science* **2002**, *295*, 483–485.
- Reimers, C. E.; Tender, L. M.; Ferig, S.; Wang, W. Harvesting energy from the marine sediment-water interface. *Environ. Sci. Technol.* **2001**, *35*, 192–195.

- (21) Chaudhuri, S. K.; Lovley, D. R. Electricity generation by direct oxidation of glucose in mediatorless microbial fuel cells. *Nat. Biotechnol.* **2003**, *21*, 1229–1232.
- (22) Min, B.; Logan, B. E. Continuous electricity generation from domestic wastewater and organic substrates in a flat plate microbial fuel cell. *Environ. Sci. Technol.* **2004**, *38*, 5809–5814.
- (23) Rabaey, K.; Sompel, K. V.; De Maignien, L.; Boon, N.; Aelterman, P.; Clauwaert, P.; Schampelaere, L.; De Pham, H. T.; Vermeulen, J.; Verhaege, M.; Lens, P.; Verstraete, W. Microbial fuel cells for sulfide removal. *Environ. Sci. Technol.* **2006**, *40*, 5218–5224.
- (24) Kim, J. R.; Cheng, S.; Oh, S.-E.; Logan, B. E. Power generation using different cation, anion and ultrafiltration membranes in microbial fuel cells. *Environ. Sci. Technol.* **2007**, *41*, 1004–1009.
- (25) Logan, B. E.; Regan, J. M. Microbial fuel cells—challenges and applications. *Environ. Sci. Technol.* **2006**, *40*, 5172–5180.
- (26) Lovley, D. R.; Phillips, E. J. P. *Appl. Environ. Microbiol.* **1986**, *51*, 683–689.
- (27) Liu, H.; Cheng, S.; Logan, B. E. Power generation in fed-batch microbial fuel cells as a function of ionic strength, temperature, and reactor configuration. *Environ. Sci. Technol.* **2005**, *39*, 5488–5493.
- (28) Williams, A. G. B.; Scherer, M. M. Spectroscopic evidence for Fe(II)-Fe(III) electron transfer at the iron oxide-water interface. *Environ. Sci. Technol.* **2004**, *38*, 4782–4790.
- (29) Tender, L. M.; Reimers, C. E.; Stecher, H. A.; Holmes, D. E.; Bond, D. R.; Lowy, D. A.; Pilobello, K.; Fertig, S. J.; Lovley, D. R. Harnessing microbially generated power on the seafloor. *Nat. Biotechnol.* **2002**, *20*, 821–825.
- (30) Shantaram, A.; Beyenal, H.; Rannjan, R.; Veluchamy, A.; Lewandowski, Z. Wireless sensor powered by microbial fuel cells. *Environ. Sci. Technol.* **2005**, *39*, 5037–5042.
- (31) Jeon, B. H.; Dempsey, B. A.; Royer, R. A.; Burgos, W. D. Low-temperature oxygen trap for maintaining strict anaerobic conditions. *J. Environ. Eng.* **2004**, *130* (11), 1407–1410.
- (32) Liu, H.; Logan, B. E. Electricity generation using an air-cathode single chamber microbial fuel cell in the presence and absence of a proton exchange membrane. *Environ. Sci. Technol.* **2004**, *38*, 4040–4046.
- (33) Zhao, F.; Harnisch, F.; Schröder, U.; Scholz, F.; Bogdanoff, P.; Herrmann, I. Application of pyrolysed iron (II) phthalocyanine and CoTMPP based oxygen reduction catalysts as cathode materials in microbial fuel cells. *Electrochem. Commun.* **2005**, *7*, 1405–1410.
- (34) Zuo, Y.; Cheng, S. A.; Call, D.; Logan, B. E. Tubular membrane cathodes for scalable power generation in microbial fuel cells. *Environ. Sci. Technol.* **2007**, *41*, 3347–3353.
- (35) Logan, B. E.; Cheng, S. A.; Watson, V.; Estadt, G. Graphite fiber brush anodes for increased power production in air-cathode microbial fuel cells. *Environ. Sci. Technol.* **2007**, *41*, 3341–3346.

ES0712221